Rit Veðurstofu Íslands

Reynir Böðvarsson
Sigurður Th. Rögnvaldsson
Ragnar Slunga
Einar Kjartansson

The SIL data acquisition system - at present and beyond year 2000

VÍ-R98005-JA04
Reykjavík
September 1998

ISSN 1025-0565
ISBN 9979-878-12-6

Reynir Böðvarsson
Sigurður Th. Rögnvaldsson
Ragnar Slunga
Einar Kjartansson

The SIL data acquisition system - at present and beyond year 2000

VÍ-R98005-JA04
Reykjavík
September 1998

CONTENTS

1 SUMMARY

The South Iceland Lowland (SIL) data acquisition system presently consists of 33 digital, three component seismic stations connected to a common data center. The automatic, on-line, earthquake analysis performed by the SIL network can be divided into three categories: *Single-station analysis* performed at the site stations producing information about all incoming phases. A short message with data on the phase is sent to the center. *Multi-station analysis* done at the center, using the phase reports from the stations and producing information about all detected events including estimates of location, magnitude and fault plane solutions. *Alert reporting* to notify the operators of the network in cases of a priori defined changes in parameters derived from the single- and multi-station analysis. The system is designed for maximum automatic operation and minimum operational cost and has shown to be capable of automatic evaluation of more then 1000 earthquakes per day or episodically several earthquakes per minute. While no attempt is made to detect and locate teleseismic events, teleseismic data is automatically saved, based on email messages from global seismological networks. Groups of events are analyzed using correlation techniques to obtain accurate absolute and relative locations of earthquakes with similar waveforms. In some areas within the network most of the earthquakes correlate very highly with each other. Based on this a new approach is being taken regarding the automatic operation of the network. A geographically indexed database will be created where different classes of earthquakes are stored. As new earthquakes are recorded by the network the system automatically looks for similar waveforms in this database and, if found, takes the onset and first motion direction picks from there. The algorithm is planned to be implemented in late 1999. New methods have been developed to estimate the stress tensor based only on the microearthquake focal mechanisms and accurate relative locations. This is planned to be implemented into the automatic on-line procedures. Methods and related software are being developed for real-time monitoring of fault movements based on the high accuracy locations and fault plane solutions.

2 INTRODUCTION

In 1980 the Council of Europe set up a working group, Comité Ad Hoc d'experts pour les Recherches sur les Tremblements de terre (CAHRT), to prepare an earthquake prediction programme for Europe. CAHRT finalized its work in 1983. A central suggestion in CAHRT's resolution was a multinational concerted effort of earthquake prediction research in five specified test areas in Europe. The South Iceland Lowland (SIL) was one of these test areas. The SIL is transected by the South Iceland seismic zone (SISZ), a transform zone connecting the on-land continuation of the Reykjanes ridge (RR in Figure 1) and the eastern rift zone (ERZ in Figure 1). A second transform, the Tjörnes fracture zone (TFZ), connects the north end of the ERZ and the Kolbeinsey ridge (KR) off-shore northern Iceland. The largest earthquakes in the SISZ exceed magnitude 7 and have recurrence intervals of the order of 100 years. The last major earthquakes sequence in the SISZ was in 1896 and a single $M = 7$ event occurred there in 1912 (Einarsson et al. 1981).

Based on the European initiative, the Nordic countries in 1988 started a project on earthquake prediction research in southern Iceland called the SIL project (Stefánsson et al. 1993). The main achievement of the SIL project was to establish an automatic earthquake data acquisition and evaluation system, the SIL system. As detailed plans were made for the SIL project the importance of microearthquakes in earthquake prediction research and their significance for understanding the physical processes leading to earthquakes were generally recognized. It was

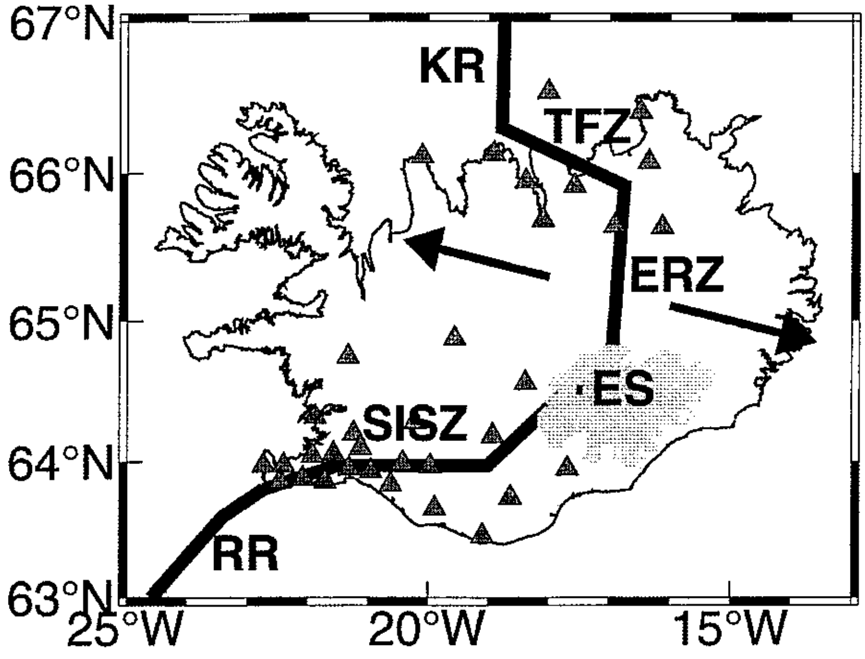

Figure 1. *The main tectonic features in Iceland. The two transform zones, the South Iceland seismic zone (SISZ) and the Tjörnes fracture zone (TFZ), connect the eastern rift zone (ERZ) to the Reykjanes ridge (RR) and Kolbeinsey ridge (KR). Arrows indicate the plate motion. Stations of the SIL network are denoted by triangles. Vatnajökull glacier is in grey, ES is the site of the 1996 subglacial eruption.*

recognized that the recording of earthquakes down to magnitude $M_L = 0$ and retrieval of source information from these events would require a new seismic network design. The rapid evolution in computer and communication technology and the introduction of inexpensive but powerful personal computers allowed for such a design of the SIL network.

The first eight stations of the new seismological network were installed in the South Iceland seismic zone in 1990. Since then 13 stations have been added in South Iceland, 9 stations in North Iceland and additionally 3 in the central part of Iceland, making a total of 33 stations (Figure 1). More than 100000 microearthquakes have been recorded and analyzed by the network during the operational period 1990 through 1997.

The major goals for the design of the system were to minimize the investment and operational cost of the system while retaining full detection capabilities and highest possible data quality (Stefánsson et al. 1986; Böðvarsson 1987). To achieve this, the system operation is highly automatic in order to minimize the analyst's workload and utilizes intelligent site stations to minimize data transmission cost. A detailed description of the SIL system is given by Böðvarsson et al. (1996). The system has been further developed within the project Earthquake-Prediction Research in a Natural Laboratory (PRENLAB) supported by the European Commission within the 4th framework of Environment and Climate Programme. In this paper we give an overview of the present version of the data acquisition system and describe some of the enhancements currently being worked on. New features of the system include a geographically indexed database, stress tensor inversion software, interactive tools for fault movements analysis and the continuous ground motion monitoring software. Some of these concepts have been implemented while others are under development.

3 AUTOMATIC ANALYSIS IN THE SIL SYSTEM

The remote stations of the SIL acquisition system are connected to a data center in Reykjavík through an X.25 link. Each station is equipped with a three-component seismometer, a 16 bit gain-ranging digitizer, a GPS synchronized clock and a 32 bit personal computer (PC) running the UNIX operating system. The data is initially sampled at 400 samples per second and is then digitally filtered and decimated down to 100 samples per second. The sampling is done synchronous to the UTC time. The dynamic range of the system is 136 dB. The gain accuracy of the digitizer is better than 0.1% (Böðvarsson et al. 1996). The velocity response of the digitizer and the different geophones currently in use is shown in Figure 2.

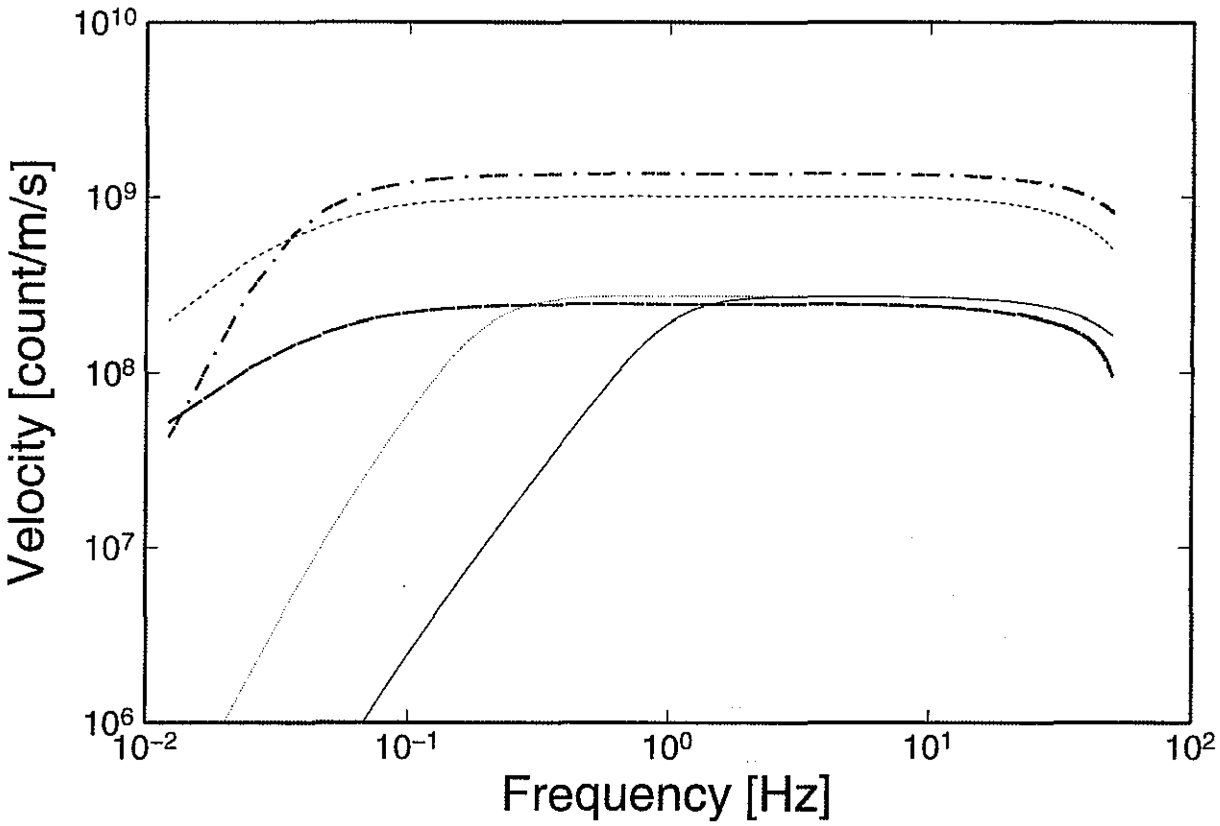

Figure 2. *The frequency response of the digitizer and 5 different geophones currently used in the SIL network. Solid line is for the Lennartz LE1, dotted line is Lennartz LE5, thick dashed line is Streckheisen STS-2, thin dashed line is Guralp 3T and the thick dashed-dotted line is for the Guralp 3T-ESP sensor. Lennartz LE1 and LE5 are used at 8 and 14 stations, respectively, Guralp 3T at 8 stations and 3T-ESP at 2 stations and 1 station is equipped with an STS-2 sensor.*

The automatic analysis performed by the SIL system can be divided into single- and multi-station analysis, multi-event analysis and the alert analysis. Single-station analysis is performed at each site on data recorded by that station. Multi-station and multi-event analysis is done at the center where data from more than one station are available. The alert monitoring is also done at the center, using parameters derived from the single- and multi-station analysis. A schematic description of the data flow in the SIL system is given in Figure 3.

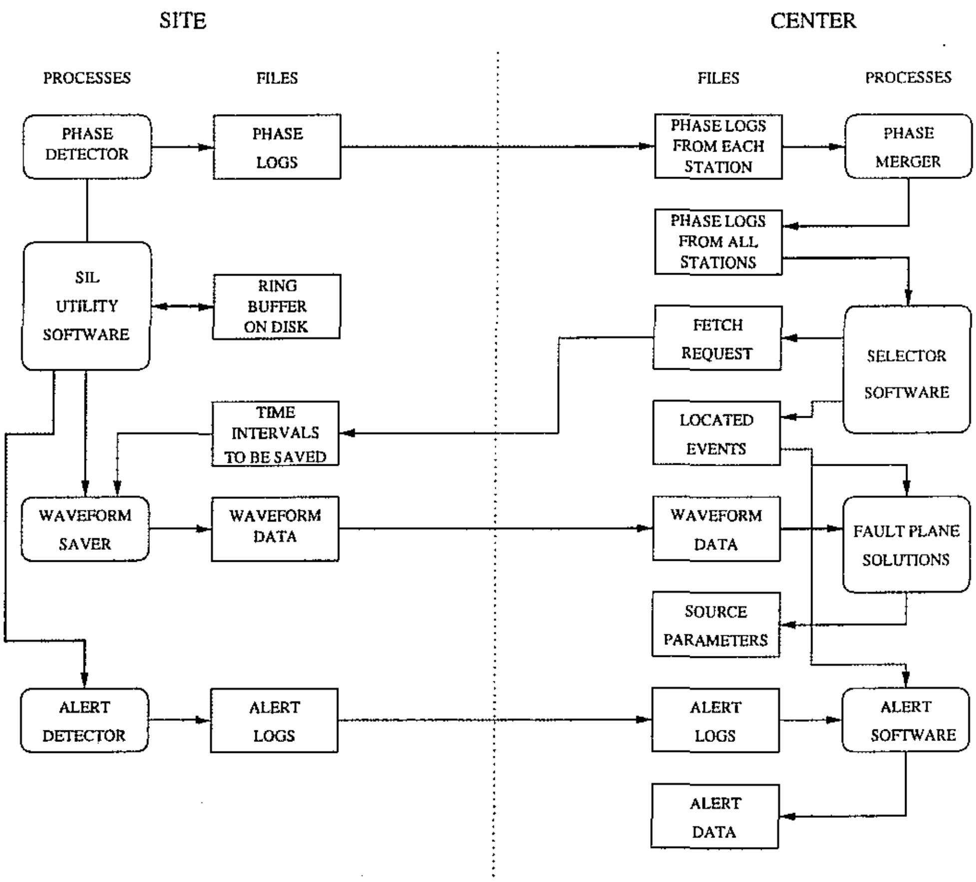

Figure 3. *Flow chart of SIL processing. The phase detector at the site produces phase logs which are transferred to the center. At the center a programme merges phases from all stations to one file which is input to the "selector" software. The selector software defines possible events through a phase association procedure and determines time intervals of waveform data to be retrieved from the site stations. At the stations the net-saver programme copies the data from the ring buffer system to local files and transfers them to the center. The alert software works in parallel with the acquisition system using information from the selector software and from the alert detector at each site. Modified from Böðvarsson et al. (1996).*

3.1 Processing at the site stations

The software at the site can be divided into two categories: utility processes and application processes. The utility processes are general data management processes, designed for flexibility and valid for any type of data acquisition. The application processes read a channel of data stream as if it were an endless file. Channels are opened as regular files would be, by a call to the specific function in the utility library. The most recent part of the data are kept in shared memory for fastest possible access.

The communication between the center and the stations is designed to be independent of the physical way the communication is realized. UNIX utilities are used throughout, providing the best possible portability of the software.

To minimize data transmission costs the SIL system uses single-station phase detections and multi-station event selection. The basis of this concept is to treat all transients detected at the stations as if they were phases associated with real earthquakes. The detector uses a simple comparison of power in two adjacent windows of the seismic trace. This is similar to the STA/LTA approach but in this case the time-windows used are both of the same length. Selected windows around the detected transients are processed in a manner one would process a true seismic phase and the results stored in a compact structure, called a phase log. Each phase log entry is only 128 bytes long and is therefore inexpensive to transmit to the center. The detection thresholds can therefore be set very low, allowing smaller earthquakes to be detected. The phase logs are transmitted to the center immediately after detection. Each phase log includes onset time, duration, reference to previous and following phases, type of phase (P or S), signal and noise averages, maximum amplitude, azimuth and coherency (Roberts et al. 1989) and spectral parameters including DC-level and corner frequency. The coherency is a measure of the linearity in the polarization of a seismic signal and should thus be high for P waves. This is not the case for most events recorded by the SIL network. The polarization information is rather unstable and this was observed already when the first station was installed. To investigate this, several mobile stations where deployed in 1992 in the vicinity of a station in the WVZ exhibiting extreme nonlinearity. Nonlinear polarization of the P wave was found at all the temporary sites (Bryndís Brandsdóttir 1998, pers. comm.). Polarization analysis of data from the first eight stations in the SIL network was performed 1990 and the results showed unstable results for most earthquakes due to lack of energy on the horizontal components for P waves. Therefore the distinction between P and S phases is made based on the amplitude ratios between the vertical and horizontal components. This method works well for approximately 60% of the used phases. Artificial neural networks are used to obtain additional information for distinguishing between the P and S phases. The learning set for the neural network was taken from the manually checked database at the center. The inputs to the neural net are the amplitude and frequency information and the coherency measure from three component analysis in the phase log. The output is set to 0 for P and 1 for S. The neural network increases the correct identification to over 95% of the used phases (Figure 4). This is very important for the phase association procedure in the multi-station analysis.

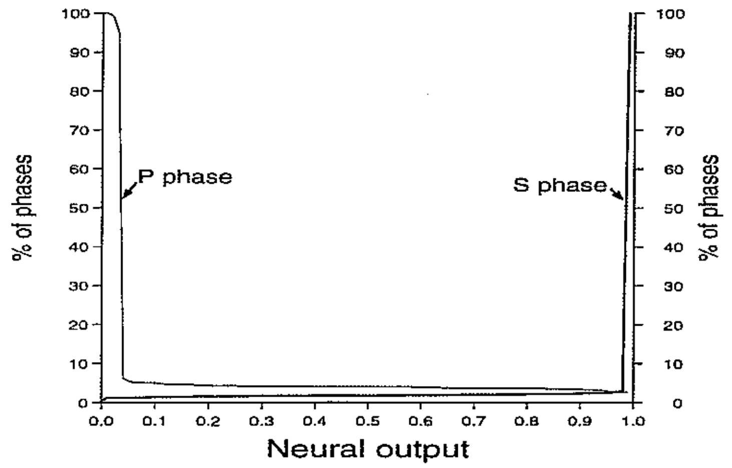

Figure 4. *The results of an artificial neural network trained to distinguish between P and S phases. A value of the neural output close to 0 indicates an P phase and a value close to 1 indicates an S phase. An intermediate value means that the phase could not be classified as either P or S. The neural network correctly identifies over 95% of the used phases.*

3.2 Processing at the center

3.2.1 Phase association and event location

Selection of waveform data to be transferred from the stations is carried out automatically by the selector software at the center. At the center, the phase logs from different stations are merged into a single time-ordered list. The first step of the selection process is to search for time intervals which contain two or more phase detections that may originate from the same seismic source. The phase detections in this time interval are then submitted to the iterative location, phase association and phase truncation procedure as explained below.

The principles for the step from a list of phase detections to a list of earthquakes or seismic events are described by Slunga (1980). In short each combination of three observations (onset times of P or S phases and azimuths of P phases) is taken as defining the initial location of an earthquake and is then followed by iterative location and phase association and truncation. This procedure may lead to a "kinematic event" (no dynamic constrains) defined by three or more observations. The list of kinematic events contains a large proportion of false events due to random coincidences of observations. Therefore each event is assigned a quality measure. Ideally the quality of an event should measure the probability that the event is a true seismic event. The computation of quality is based on both kinematic considerations and analysis of the amplitudes of the detected phases (dynamic information). Negative evidence (i.e. lack of detections) has proved to be most valuable for local and regional networks due to the strong distance dependency of the amplitudes of seismic waves at the distances involved. The kinematic contribution to the event quality is proportional to the square of the number of P and S arrivals used in the location of the event. Stations not observing the event will reduce the event quality if the event size and observing distance is such that one would expect a detection. In a similar way stations that have kinematic detections but which are not expected to detect the event will reduce the event quality. The size of the reduction depends on the size of the expected amplitude at the station in both cases. When computing the event quality one starts with only the closest station and computes the quality as if it is the only detecting station. Then stations are added in distance order and the quality is recalculated every time. The maximum quality during this procedure is taken as the event quality.

A new application of artificial neural networks is being tested in the phase association procedure. Information on the true phase association is extracted from the manually checked database and used as a learning set. All phases related to an event are marked "associated" and all phases detected in the time vicinity of that event are marked "not associated". The inputs to the neural net are the amplitude and frequency information from phase logs from two stations, the distance between the stations and the time difference between these phases. The first results indicate that 50% of the false or useless phases can be rejected prior to the deductive phase association procedure if accepting up to 1% loss of real and useful phases. This work is in its initial stage but we believe that the neural network approach to the phase association problem will be very valuable for the network operation.

3.2.2 Fault plane solutions

Apart from locating the earthquake, the routine analysis performed on every recorded event includes estimating fault plane solutions for the earthquake. The estimation of focal mechanism and source parameters are based on results of the spectral analysis of short data segments containing the direct P and S wave arrivals. The spectral estimation is done at the site stations, using windows around the automatic time picks, and repeated at the center after manual refinement of arrival time readings. The low frequency amplitude of each phase is determined by fitting a three parameter model to the observed spectra (Boatwright 1978). To estimate the fault plane solution for the earthquake a systematic search over strike, dip and rake is performed. For each combination of the three source angles, the misfit between observed and predicted spectral amplitudes is calculated. In addition to the single best fitting solution, all solutions that fit the observed polarities and have amplitude misfit less than a predefined threshold value are taken as acceptable (Slunga 1981). The analysis procedure is the same for all located events. However, the fault plane solutions will be better constrained for events recorded at many stations than for small earthquakes recorded only at few stations. For earthquakes within the SISZ the optimal fault plane solution can be expected to be within $\pm 15°$ of the true source angles for events larger than $M_L \sim 0.5$ (Rögnvaldsson and Slunga 1993). The corner frequency of the spectra is used to estimate the source dimensions (Boatwright 1980) and, together with the seismic moment, the peak slip at the source (Eshelby 1957) and the static stress drop (Brune 1970, 1971).

3.3 Continuous ground motion monitoring

The site station software has recently been enhanced to enable continuous monitoring of ground velocity. The signals are filtered through 3 bandpass filters that pass data in the ranges 0.5–1 Hz, 1–2 Hz and 2–4 Hz. The filters are implemented in the time-domain in real-time using the expression

$$y_k = \sum_{i=0}^{2} a_i x_{k-i} + \sum_{j=1}^{8} b_j y_{k-j}$$

where x_k is the unfiltered signal, y_k is the filtered signal and a_i and b_j are coefficients of the filter.

Each of the three components is filtered using the three filters and an average value for the amplitude is computed once a minute. The average values are sent to the center where they are stored. A near real-time plot of this data gives a useful visual indication of the seismic activity and the condition of the network. Individual earthquakes larger than about $M_L = 2$ are seen on the plots. This data can also be used to estimate local magnitude for those earthquakes (Mendi and Husebye 1994).

3.3.1 Volcanic tremor

The primary reason for developing this software was to enable the monitoring of the tremors that accompany volcanic eruptions. The software was implemented in November 1996, just after the eruption in Vatnajökull in October 1996 (Guðmundsson et al. 1997). During the eruption, data were recorded on portable Reftek instruments operated by the Hotspot project (Allen et al. 1998), as well as at the SIL stations.

Figure 5 shows tremor recorded on a temporary station at Grímsfjall, at a distance of approximately 10 km from the eruption site (Figure 1), during the eruption. Subglacial eruption probably started a few hours before midnight on September 30, beneath about 700 m of ice. Subsidence of the glacial surface was observed the following morning. Eruption activity was last observed on October 12. Only minor steam emissions were seen on October 13. The plot shows a continuous tremor that was surprisingly uniform during the eruption. Closer inspection shows

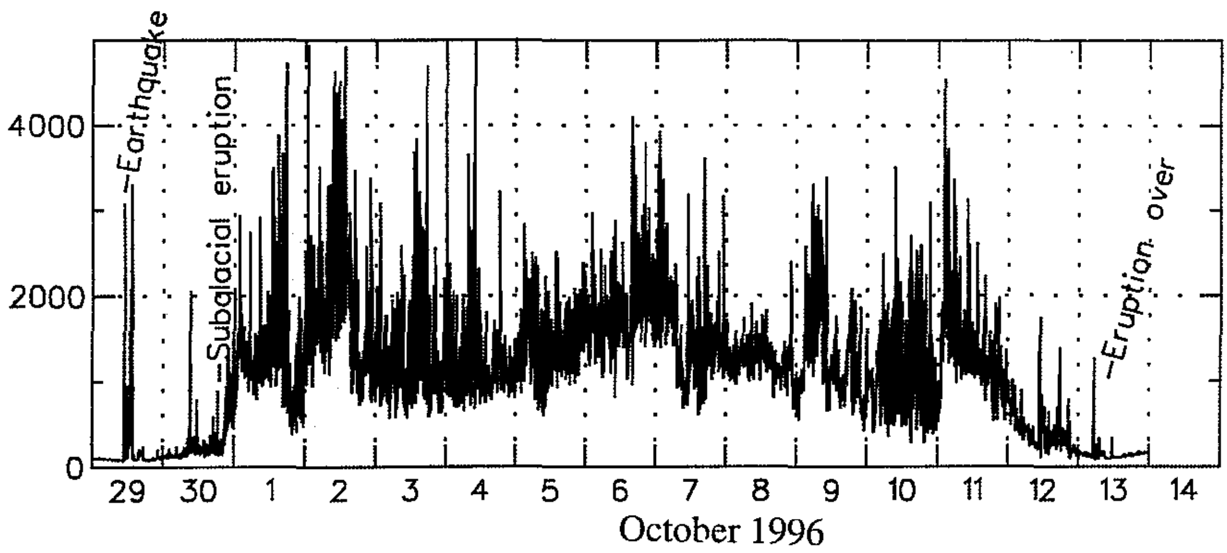

Figure 5. *Tremor in the 0.5–1.0 Hz frequency band recorded on a temporary station at Grímsfjall prior to and during the 1996 subglacial eruption in Vatnajökull.*

that superimposed on this are strong bursts that often lasted between 10 and 30 minutes.

The eruption was preceded by a magnitude 5.3 earthquake 15 km north of the eruption site. The earthquake was followed by an intense earthquake swarm. The signal seen before the start of the eruption is the result of a very intense earthquake swarm (several events per minute), possibly combined with tremor caused by magma movement.

3.3.2 Jökulhlaup

Other sources of seismic tremor include turbulent water-flow and steam explosions. Figure 6 shows tremor during a catastrophic flood that drained a subglacial cauldron, 5 km west of the eruption site, recorded on a SIL station at a distance of 45 km. Observable tremor at 1–2 Hz started at about the same time as sulphur smell was detected at several locations in South Iceland, around 9 am on August 16, 1997. The peaks are tremor bursts that were probably caused by boiling in the subglacial geothermal field, that resulted from the sudden drop in pressure when the cauldron was drained. These tremor bursts lasted up to 30 minutes and were strong enough to be observed at most SIL stations.

3.4 The alert system

The alert system is a collection of routines for monitoring extracted parameters in selected regions and sites. For this purpose, Iceland is currently divided into 29 regions and different alert thresholds assigned to each region. The parameters are extracted from the results of the analysis described above and from dedicated alert detectors at the sites. The alert system is started at regular intervals and for each event defined by the multi-station analysis. At present five parameters are monitored for each region. These are M, the local magnitude of individual earthquakes; N, the number of earthquakes in a time interval; S, a dimensionless measure of moment release during the same time interval; a time-weighted measure of the number of events

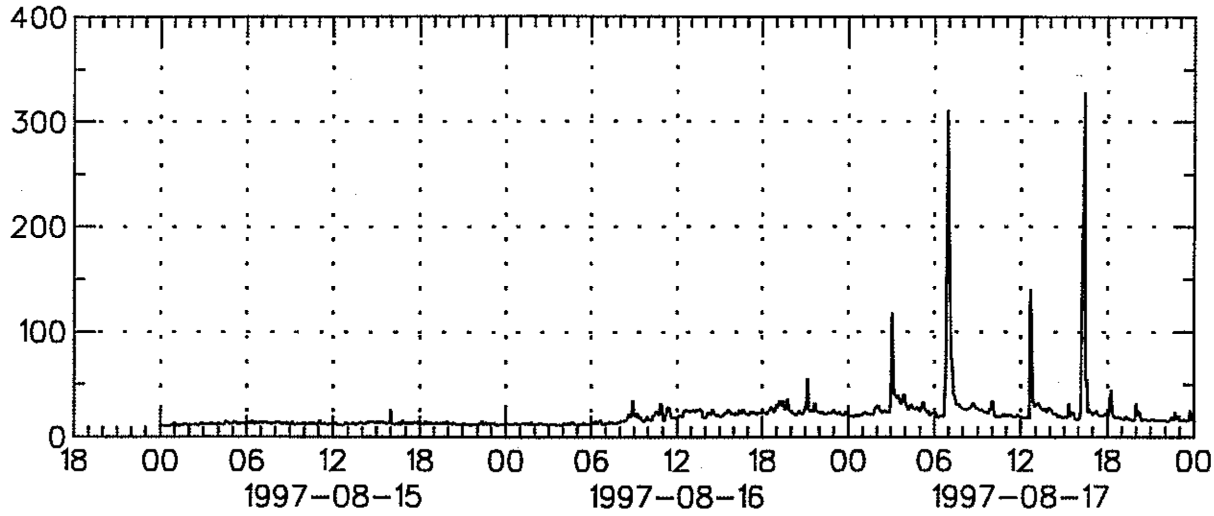

Figure 6. *Tremor during a catastrophic flood that drained a subglacial cauldron beneath the Vatnajökull glacier. The data are recorded on a SIL station 45 km away.*

and a time-weighted measure of accumulated moment release.

The dimensionless moment release parameter is defined as

$$S = \sum_{i=1}^{N} S_i = \sum_{i=0}^{N} 10^{(5+M_i)}$$

Here M_i is the magnitude of the i-th earthquake and $S_i = 10^{(5+M_i)}$ is a dimensionless measure of the seismic moment released. The form of the definition of S_i stems from the relationship between surface wave magnitude, M_s, and seismic moment, i.e. $\log M_0 = 9.1 + 1.5M_s$ and hence $M_0 = 10^{9.1+1.5M_s}$ (Purcaru and Berckhemer 1978). A time-weighted function of moment release, $S_w = \sum_{i=0}^{N} w_i S_i$, is also monitored. Here $w_i = \frac{k}{1+t_i}$ where k is a constant and t_i is the time since the occurrence of event i. Thus recent events are assigned more weight than the "older" ones.

Similarly a time-weighted function of the number of earthquakes is defined as

$$N_w = \sum_{i=0}^{N} w_i = \sum_{i=0}^{N} \frac{k}{1+t_i}$$

If any of the parameters M, N, N_w, S or S_w exceeds predefined limits, an alert level is declared.

A special detector is operated at the individual stations for the alert system. It monitors two parameters, large ground velocity and increase in background noise during some period of time.

3.5 Automatic saving of teleseisms

The SIL seismic data acquisition system was primarily designed for automatic acquisition and evaluation of data from local microearthquakes. No attempt has been made to automatically locate teleseismic events but the acquisition system is now also used for collecting teleseismic data.

The so-called "E" type messages from USGS and NEIC, containing a single line of hypocenter and magnitude information on recent earthquakes, are received via electronic mail. A selection programme reads the messages and selects events that fulfill certain criteria of magnitude and epicentral distance. The programme uses the iasp91 traveltime tables (Kennett and Engdahl 1991) to compute the first arrival time at each station. The teleseismic body wave data are fetched with a sampling rate of 20 samples per second and the surface wave data with a sampling rate of 4 samples per second. This extended use of the SIL system provides valuable data for tomography studies (Darbyshire et al. 1997; Allen et al. 1998).

4 MULTI-EVENT ANALYSIS

Multi-event analysis can be performed on groups of events within a limited hypocentral distance. This includes the relative location of groups of similar events resulting in very accurate hypocenter location, and inversion of the fault planes and the slip direction for the stress tensor. Steps are being taken towards real-time monitoring of unstable faults.

4.1 Multi-event absolute and relative locations

It is well established that accurate measurements of the arrival time difference between similar earthquakes can be used to constrain the relative locations of the quakes. The arrival time differences are measured through cross-correlation of the seismograms. The most common approach is to select one event from the earthquake cluster as a reference or master event and measure arrival time differences of the other earthquakes relative to the master event (e.g. Deichmann and Garcia-Fernandez 1992; Ito 1985; Console and Giovambattista 1987; Frémont and Malone 1987). A more complete approach is to measure the arrival time differences between each event and all the others, i.e. every earthquake in the group is used as a "master event" (Slunga et al. 1984, 1995; Got et al. 1994; Shearer 1997).

The timing accuracy achieved by cross-correlation techniques can also be used to improve the absolute locations of groups of earthquakes. The main sources of error when locating with time differences of similar events are the uncertainties in the ray directions in the source volume. The deviations of ray directions from those predicted by the 1D velocity model are partly independent of the integrated travel time error along the path. This means that the absolute location errors from the use of arrival time differences are nearly independent of the single-event location errors (Slunga et al. 1995).

At the SIL center the algorithm described by Slunga et al. (1995) is used to simultaneously determine absolute and accurate relative locations of clusters of similar earthquakes. An example of the application of the relative location algorithm to a group of earthquakes in the Tjörnes fracture zone (Figure 1) is shown in Figure 7. After relocation the epicenters of the 18 successfully located events lie on an approximately 1 km long line segment (Figure 7a). Assuming that all the earthquakes occurred on the same fault, the attitude of the fault can be estimated by fitting a plane through the accurately determined hypocenters. The strike of the best fitting plane through the group is N139°E, similar to the strike of the main transform faults of the TFZ. The best fitting plane dips 84°. The mean distance of the 18 earthquakes from the plane is 11 m, comparable to the uncertainty in the relative locations. The normals to all planes which can be fit through the hypocenter cluster with mean distance of the hypocenters from the plane less than 50 m are shown in Figure 7c on an equal area projection of the lower hemisphere. Clearly the acceptable (according to our definition) plane orientations are confined to a narrow range (approximately $\pm 10°$ in strike and $\pm 20°$ in dip) around the best fitting orientation.

This method has been used to map active faults in the two transform zones in South and North

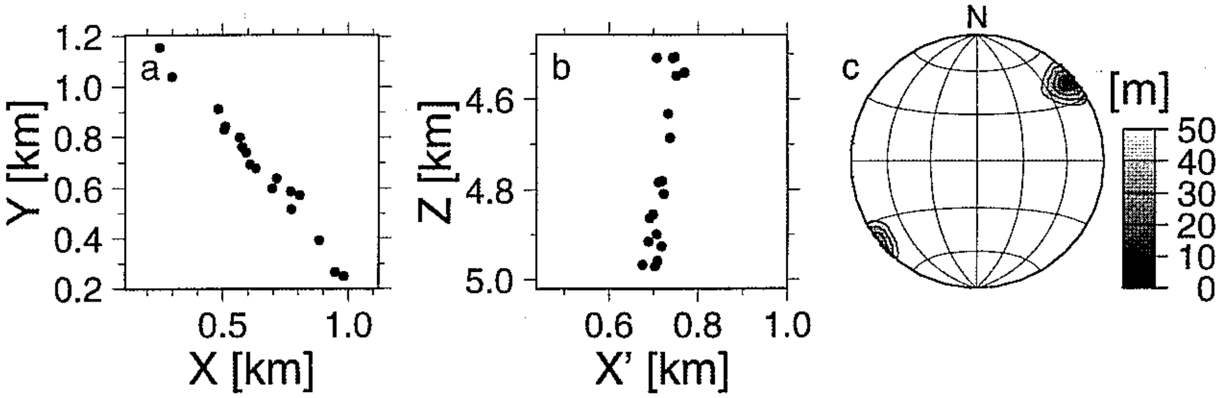

Figure 7. *The relative location of a group of 18 earthquakes in the Tjörnes fracture zone. (a) shows a mapview of the epicenters after relocation, X is east, Y is north. In (b) the hypocenters are viewed along the strike of the best fitting plane through the group. Z is depth and X' is horizontal and orthogonal to the strike. (c) shows the poles to all planes through the hypocenter group, such that the mean distance of the 18 earthquakes from the plane is less than 50 m, plotted on an equal area projection of the lower hemisphere.*

Iceland, as well as at the divergent plate boundaries in SW-Iceland (Rögnvaldsson and Slunga 1994; Slunga et al. 1995; Rögnvaldsson et al. 1996, 1998). The attitudes of active faults at depth generally agree well with observations of surface faults. As more earthquake clusters are analyzed in this manner, data on mapped subsurface faults are collected in a database at the SIL center. The data are accessible over the Internet at http://www.vedur.is/~sr/faults.html. This database currently holds the results of analysis of more than 100 swarms.

4.2 Automatic reading of onset and first motion direction

Based on the positive results of the correlation techniques used in the relative location algorithm a new approach is being taken regarding the automatic operation of the network. Experience shows that a substantial fraction of the events occurring within a given area belongs to a few clusters or families of earthquakes, characterized by highly similar waveforms. The cross-correlation of seismograms at individual stations can be used to identify such clusters of similar events (e.g. Aster and Scott 1993; Maurer and Deichmann 1995). We are currently working on a method for using cross-correlation of neighboring events to automatically determine the onsets of P and S phases with accuracy comparable to or better than achieved in the interactive analysis. The aim is to reduce the need for manual inspection of seismograms from local and regional earthquakes and to improve the quality of the readings in the microearthquake database. We plan to implement a first version of this software in 1999.

The objective is to create a geographically indexed database (GID) where different classes of earthquakes will be stored. The area to be covered by the database is divided into equidimensional cells, 2×2 km^2 laterally but of unconstrained depth. When creating the GID, each event within a given cell is correlated with all other earthquakes in the cell. The results of the correlation are used to group the earthquakes into classes. A few events of each class are stored in the GID.

As new earthquakes are recorded by the network, the system automatically looks for similar waveforms in the GID. The initial location estimate of the event is used when accessing the GID. The selection of waveform windows to be compared to data in the GID is done based on the automatically determined arrival times for stations that detected the phase. At other close stations that did not detect the phase, theoretical arrival times are estimated by ray-tracing through a layered velocity model.

The new phase is correlated with all phases of the same type (P or S) in the GID, recorded at the same station and originating within the same cell or a neighboring cell. The cross-correlation function (CCF) is resampled before determining the time lag, the correlation coefficient and the sign of the CCF at the peak. The lag gives the absolute arrival time of the phase, assuming the reference pick was "correct". If the polarity of the reference phase is known, the sign of the CCF gives the polarity of the new phase. The normalized correlation coefficient gives a measure of the similarity of the new phase to the reference phase. By resampling the CCF the accuracy of the pick is practically only limited by the timing accuracy of the network clocks. For the timing in the SIL system this is better than 1 ms. The precise arrival time readings can also be used for determining accurate relative locations of similar earthquakes.

When all recorded phases for the new event have been compared to all relevant phases in the GID, a voting procedure is used to determine whether the event is similar to sufficiently many phases in the database to warrant skipping interactive analysis. If enough phases have been picked by correlation with existing phases, the picks are written to a file similar to those created in the interactive time picking procedure and the event is relocated using the correlation picks. Otherwise the new event is analyzed interactively by the network operators. Figure 8 gives a schematic overview of data flow in the proposed correlation analysis system.

4.3 Stress tensor inversion

New methods and software have been developed to estimate a regional or local stress tensor based only on microearthquake focal mechanisms and locations. The inversion scheme is based on existing techniques (Gephart and Forsyth 1984) which have been improved along two major lines:

1. The method takes advantage of the SIL fault plane solution algorithm and is thus able to handle a range of acceptable fault plane solutions for each event. This is a reasonable way of handling the uncertainty in the fault plane solutions. The stress tensor is in this case used as an intermediate parameter for joint fault plane solutions.

2. The crucial point of choosing the proper fault plane, is tackled both the traditional way, by goodness of fit between observed slip and estimated shear stress direction (Gephart and Forsyth 1984), and with two new approaches. The fault plane can be chosen as the one least stable, using a simple Mohr-Coulomb criterion, in the tested stress regime using the stress tensor as an intermediate parameter, or with information from the SIL system fault mapping algorithm for absolute and relative location.

The software has been developed and implemented in the SIL system context. Tests with synthetic data, semi-synthetic (geological) data and real data from the SIL area have shown good performance of the methods (Lund and Slunga 1998). The algorithms will be implemented into the automatic on-line analysis.

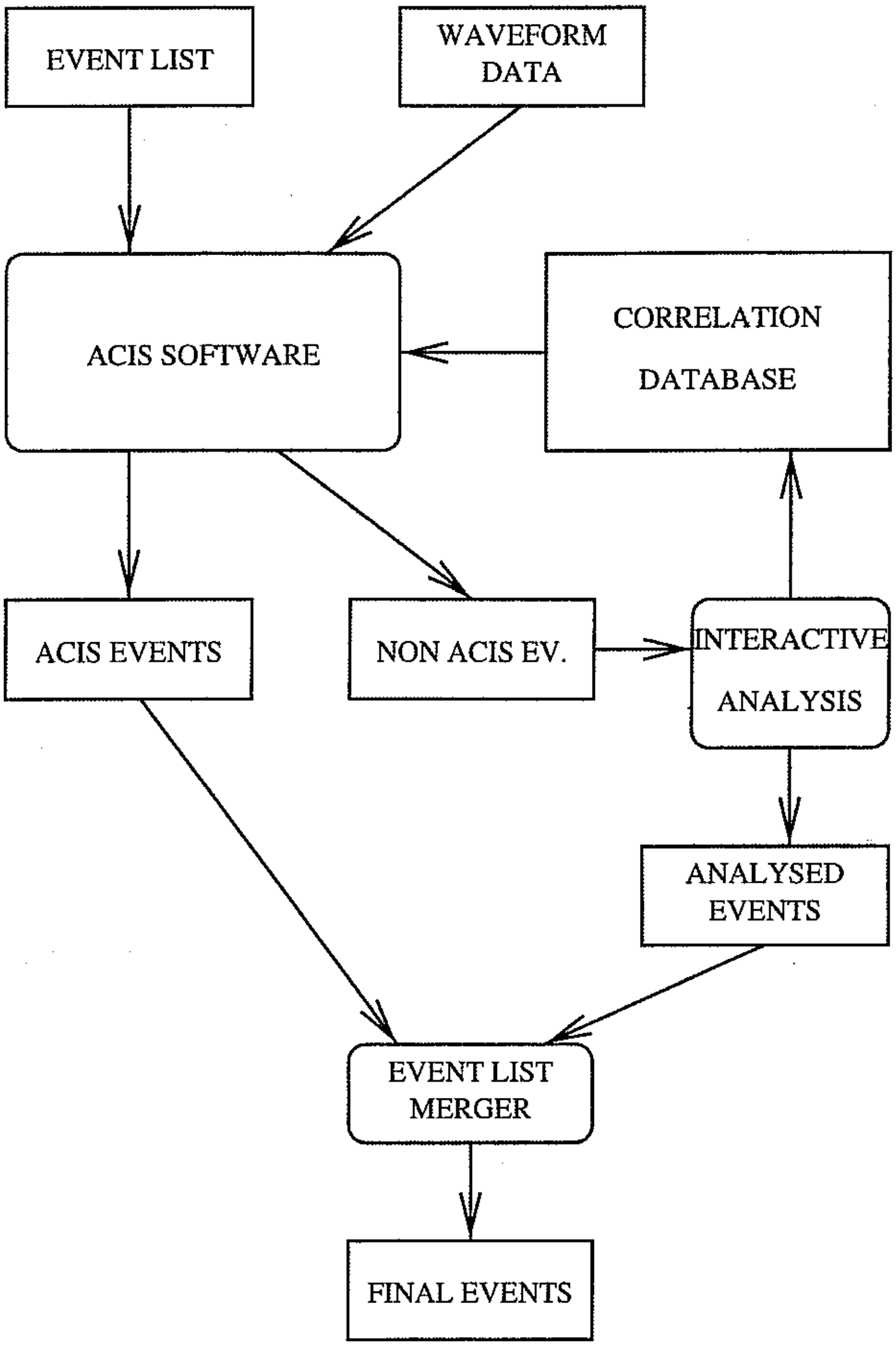

Figure 8. *A simplified flowchart of the automatic cross-correlation procedure. Programs are surrounded by oval boxes, files by square boxes. ACIS stands for Automatic Correlation of Incoming Signals. See text for discussion.*

4.4 Real-time monitoring of fault movements

It has been generally recognized that brittle fault slip may be stable and not only unstable as in earthquakes (Tse and Rice 1986; Dodge et al. 1996; Lyakhovsky et al. 1997). The commonly observed time clustering of microearthquakes, often over distances large compared to the earthquake sizes, is probably sometimes related to deformation expressed by stable brittle aseismic slip on faults.

The present system produces absolute and high accuracy relative locations for selected groups of events. Fault plane solutions and dynamic source parameters for all detected microearthquakes are estimated in near real-time (within a few minutes of the earthquake). Based on both the relative locations and the fault plane solutions one can conclude on which fracture the earthquake slip occurred. This makes it possible to monitor the movements of the faults and fractures, identified by the multi-event locations described above, if detectable microearthquakes are generated by the fault slip. This is one of the ideas behind the PRENLAB project, as it has been suggested that slip weakening may be important in the geomechanical process leading to major earthquakes (Tse and Rice 1986). This means that in such cases a major earthquake will be preceded by a phase of accelerating stable fault slip. If this slip is indirectly detected and followed by the microearthquake activity it opens a possibility for earthquake warning before a major earthquake.

The plan is to implement algorithms for real-time monitoring of fault movements early year 2000, after the method and software developments within the PRENLAB projects.

5 DISCUSSION AND CONCLUSIONS

More than 100000 microearthquakes have been recorded during the operational period of the SIL system from 1990 to 1997. In this period the system has been developed further and the number of stations has been increased from 8 to 33 with variable station spacing.

One of the assumptions governing the design of the SIL system was that microearthquakes down to $M_L = 0$ would provide useful information for the study of larger earthquakes. The results of the work on relative locations of microearthquakes recorded by the SIL network validate this assumption. In general faults mapped by accurate relative locations and fault plane solutions for $M_L = 0$–2 earthquakes have attitudes similar to those of nearby faults that have ruptured in M = 6–7 earthquakes.

Information on the earthquake sources carried by the seismic waves is retrieved and processed automatically by the system. The high degree of automatization achieved in the SIL system makes it a good near real-time monitor of earthquake activity. Estimation of locations and source parameters for earthquakes down to magnitude below zero would be impossible without extensive automatization. More than 1200 earthquakes have been recorded and automatically analyzed by the network during one single day.

The waveform data from the SIL network are available in ah-format on request. Lists of earthquake origin times, hypocenter locations and magnitudes are available on the Icelandic Meteorological Office home page at http://www.vedur.is. These lists are updated weekly.

In 1999 we hope to implement the automatic onset and first motion direction estimation through the use of a geographically indexed correlation database. We believe that this will both decrease the workload of the persons responsible of the daily operation of the network and increase the quality of the created database. Stress tensor inversion algorithms will be implemented for automatic operation in the near future and around the new millennium we plan to have real-time fault movement monitoring connected to the alert features of the network.

Acknowledgements

The SIL project was financed by the Nordic Council of Ministers, the research councils in the Nordic countries and the Icelandic Meteorological Office. This research was financed by the European Commission Environment and Climate Programme, contract ENV4-CT96-0252, the Swedish Environmental Protection Agency, contract 011-047-97-01, and the Icelandic Research Council, grant 957010096.

6 REFERENCES

Allen, R.M., G. Nolet, W.J. Morgan, K. Vogfjörð, B.H. Bergsson, P. Erlendsson, G.R. Foulger, S. Jakobsdóttir, B.R. Julian, M. Pritchard, S. Ragnarsson and R. Stefánsson 1998. Iceland's thin hot plume. *Geophys. J. Int.*, submitted.

Aster, R.C. and J. Scott 1993. Comprehensive characterization of waveform similarity in microearthquake data sets. *Bull. Seism. Soc. Am.* 83, 1307–1314.

Boatwright, J. 1978. Detailed spectral analysis of two small New York State earthquakes. *Bull. Seism. Soc. Am.* 68, 1117–1131.

Boatwright, J. 1980. A spectral theory for circular seismic sources; simple estimates of source dimension, dynamic stress drop and radiated seismic energy. *Bull. Seism. Soc. Am.* 70, 1–27.

Brune, J.N. 1970. Tectonic stress and the spectra of seismic shear waves from earthquakes. *J. Geophys. Res.* 75, 4997–5009.

Brune, J.N. 1971. Correction. *J. Geophys. Res.* 76, 5002.

Böðvarsson, R. 1987. *Design of the data acquisition system for the South Icelandic Lowland (SIL) project.* Report, Veðurstofa Íslands, Reykjavík.

Böðvarsson, R., S.Th. Rögnvaldsson, S.S. Jakobsdóttir, R. Slunga and R. Stefánsson 1996. The SIL data acquisition and monitoring system. *Seism. Res. Lett.* 67, 35–46.

Console, R. and R.D. Giovambattista 1987. Local earthquake relative location by digital records. *Phys. Earth Planet. Inter.* 47, 43–49.

Darbyshire, F.A., K.F. Priestley, R.S. White, G. Guðmundsson, S. Jakobsdóttir and R. Stefánsson 1997. The crustal structure of northeastern Iceland: constraints from broadband teleseismic body waves. In: Abstracts from the AGU 1997 fall meeting, San Francisco, USA, December 8–12 1997. *EOS* 78.

Deichmann, N. and M. Garcia-Fernandez 1992. Rupture geometry from high-precision relative hypocenter locations of microearthquake clusters. *Geophys. J. Int.* 110, 501–517.

Dodge, A.D., G.C. Beroza and W.L. Ellsworth 1996. Detailed observations of California foreshock sequences: implications for the earthquake initiation process. *J. Geophys. Res.* 101, 22371–22392.

Einarsson, P., S. Björnsson, G. Foulger, R. Stefánsson and Þ. Skaftadóttir 1981. Seismicity pattern in the South Iceland seismic zone. In: D.W. Simpson and P.G. Richards (editors), Earthquake prediction — an international review. *Maurice Ewing series* 4. AGU, Washington, D.C., 141–151.

Eshelby, J.D. 1957. The determination of the elastic field of an ellipsoidal inclusion and related problems. *Proc. Roy. Soc. London* 241, 276–296.

Frémont, M.-J. and S. Malone 1987. High precision relative locations of earthquakes at Mount St. Helens, Washington. *J. Geophys. Res.* 92, 10223–10236.

Gephart, J.W. and D.W. Forsyth 1984. An improved method for determining the regional stress tensor using earthquake focal mechanism data: application to the San Fernando earthquake sequence. *J. Geophys. Res.* 89, 9305–9320.

Got, J.-L., J. Fréchet and F.W. Klein 1994. Deep fault plane geometry inferred from multiplet relative relocation beneath the south flank of Kilauea. *J. Geophys. Res.* 99, 15375–15386.

Guðmundsson, M.T., F. Sigmundsson and H. Björnsson 1997. Ice–volcano interaction of the

1996 Gjálp subglacial eruption, Vatnajökull, Iceland. *Nature* 389, 954–957.

Ito, A. 1985. High resolution relative hypocenters of similar earthquakes by cross-spectral analysis method. *J. Phys. Earth.* 33, 279–294.

Kennett, B.L.N. and E.R. Engdahl 1991. Traveltimes for global earthquake location and phase identification. *Geophys. J. Int.* 105, 429–465.

Lund, B. and R. Slunga 1998. Stress tensor inversion using detailed microearthquake information and stability constraints: application to the South Iceland seismic zone. *J. Geophys. Res.*, submitted.

Lyakhovsky, V., Y. Ben-Zion and A. Agnon 1997. Distributed damage, faulting, and friction. *J. Geophys. Res.* 102, 27635–27649.

Maurer, H. and N. Deichmann 1995. Microearthquake cluster detection based on waveform similarities, with an application to the western Swiss Alps. *Geophys. J. Int.* 123, 588–600.

Mendi, C.D. and E. Husebye 1994. Near real-time estimation of magnitudes and moments for local seismic events. *Annali di Geofisica* 37, 365–382.

Purcaru, G. and H. Berckhemer 1978. A magnitude scale for very large earthquakes. *Tectonophysics* 49, 189–198.

Roberts, R.G., A. Christoffersson and F. Cassidy 1989. Real–time event detection, phase identification and source location estimation using single station three–component seismic data. *Geophys. J.* 97, 471–480.

Rögnvaldsson, S.Th. and R. Slunga 1993. Routine fault plane solutions for local and regional networks: a test with synthetic data. *Bull. Seism. Soc. Am.* 11, 1247–1250.

Rögnvaldsson, S.Th. and R. Slunga 1994. Single and joint fault plane solutions for microearthquakes in South Iceland. *Tectonophysics* 273, 73–86.

Rögnvaldsson, S.Th., G. Guðmundsson, K. Ágústsson, S. Jakobsdóttir and R. Stefánsson 1996. Recent seismicity near the Hengill triple-junction, SW-Iceland. In: B. Þorkelsson (editor) *Seismology in Europe*. Papers presented at the XXV ESC General Assembly, Reykjavík, Iceland, September 9–14, 1996. ISBN–9979–60–235–X, 461–466.

Rögnvaldsson, S.Th., Á. Guðmundsson and R. Slunga 1998. Seismotectonic analysis of the Tjörnes fracture zone, an active transfrom fault in North Iceland. *J. Geophys. Res.*, in press.

Shearer, P.M. 1997. Improving local earthquake locations using the L1 norm and waveform cross correlation: application to the Whittier Narrows, California, aftershock sequence. *J. Geophys. Res.* 102, 8269–8283.

Slunga, R. 1980. International seismological datacenter: an algorithm for associating reported arrivals to a global network into groups defining seismic events. *Technical report* C 20386–T1. Swedish National Defence Research Establishment, Sweden.

Slunga, R. 1981. Earthquake source mechanism determination by use of body–wave amplitudes - an application to Swedish earthquakes. *Bull. Seism. Soc. Am.* 71, 25–35.

Slunga, R., P. Norrmann and A.-C. Glans 1984. Baltic shield seismicity, the results of a regional network. *Geophys. Res. Lett.* 11, 1247–1250.

Slunga, R., S.Th. Rögnvaldsson and R. Böðvarsson 1995. Absolute and relative location of similar events with application to microearthquakes in southern Iceland. *Geophys. J. Int.* 123, 409–419.

Stefánsson, R., H. Bungum, R. Böðvarsson, J. Hjelme, E. Husebye, H. Johansen, H. Korhonen and R. Slunga 1986. Seismiskt datasamlingssystem för Södra Islands Lågland (seismic data acquisition system for South Iceland Lowland). Report, Veðurstofa Íslands, Reykjavík. In English with Icelandic and Swedish summaries.

Stefánsson, R., R. Böðvarsson, R. Slunga, P. Einarsson, S. Jakobsdóttir, H. Bungum, S. Gregersen, J. Havskov, J. Hjelme and H. Korhonen 1993. Earthquake prediction research in the South Iceland seismic zone and the SIL project. *Bull. Seism. Soc. Am.* 83, 696–716.

Tse, S.T. and J.R. Rice 1986. Crustal earthquake instability in relation to the depth variation of frictional slip properties. *Geophys. J. Int.* 91, 9452–9472.

ISSN 1025-0565
ISBN 9979-878-12-6

Kápumynd: Klósigar (vatnsklær)
Ljósm.: Guðmundur Hafsteinsson, veðurfræðingur